Conformation and Dynamics of DNA Confined in Slitlike Nanofluidic Channels

Douwe Jan Bonthuis,* Christine Meyer, Derek Stein,+ and Cees Dekker‡

Kavli Institute of Nanoscience, Delft University of Technology, Lorentzweg 1, 2628 CJ Delft, The Netherlands

(Received 9 March 2008; published 5 September 2008)

Using laser fluorescence microscopy, we study the shape and dynamics of individual DNA molecules in slitlike nanochannels confined to a fraction of their bulk radius of gyration. With a confinement size spanning 2 orders of magnitude, we observe a transition from the de Gennes regime to the Odijk regime in the scaling of both the radius of gyration and the relaxation time. The radius of gyration and the relaxation time follow the predicted scaling in the de Gennes regime, while, unexpectedly, the relaxation time shows a sharp decrease in the Odijk regime. The radius of gyration remains constant in the Odijk regime. Additionally, we report the first measurements of the effect of confinement on the shape anisotropy.

DOI: 10.1103/PhysRevLett.101.108303 PACS numbers: 82.35.−x, 87.80.Fe

A detailed understanding of the static and dynamic properties of DNA in confined environments is essential for the design of devices for single-molecule analysis and manipulation [1,2]. In addition, it provides better insight in natural processes like DNA packaging in viruses [3] and DNA segregation in bacteria [4]. In bulk, DNA molecules form random coils that are sphere shaped on average, with radius of gyration R_{bulk}. Upon confining DNA to a nanochannel, different regimes of confinement can be distinguished. The important length scales are the bulk radius R_{bulk}, the height of the confining channel h, and the persistence length of the molecule a. In the de Gennes regime, where $2a < h < 2R_{\mathrm{bulk}}$, the molecule still has three-dimensional orientational freedom at a short length scale, forming three-dimensional blobs, while at larger scales the molecule is flattened; see Fig. 1(c). The effect of confinement on the diffusion constant in this regime has been investigated optically in slitlike nanochannels [5]. Using the same technique, the extension, diffusion constant, and relaxation time were measured in tubelike confinement [6,7]. When the height of the nanochannel reaches the persistence length ($h \approx 2a$), the orientation of the molecule becomes restricted even at the shortest length scales, drastically affecting the response of the molecule to confinement. The onset of this Odijk regime has been reported for tubelike nanochannels [6], while truly two-dimensional polymers were investigated much earlier, by adsorbing them on a lipid membrane [8]. However, an assessment of the radius of gyration of DNA in slitlike confinement, which is crucial for size separation schemes [5,9], has been lacking so far.

In this Letter, we present measurements of the radius of gyration and shape anisotropy of DNA confined to slitlike nanochannels varying in height from 33 nm to 1.3 μm. Our measurements show three regimes of DNA conformations: compression, elongation, and saturation. At $h \approx$ 100 nm, we see a strong discontinuity in the scaling of the radius of gyration and the relaxation time, which we interpret as the transition from the de Gennes to the Odijk regime.

We studied λ-phage DNA (48 kb, double-strand), stained with YOYO-1 (Molecular Probes), at a ratio of YOYO-1 to base pair of 1:6. The DNA was suspended at a concentration of 50 pg μl^{-1} in 50 mM NaCl in aqueous solution with 10 mM tris-ethylenediaminetetraacetic acid (EDTA) and 0.07% per volume dimethylsulfoxide (DMSO). The stained DNA has a persistence length of $a \approx$ 66 nm and a contour length of $\sim$22 μm [10]. The labeled molecules were illuminated by a 200 mW, 488 nm laser (Coherent). The illumination time was reduced to $\sim$100 μs using an acousto-optical modulator (A-A Opto-Electronic). We used a 100× oil-immersion objective (Olympus) with a numerical aperture of 1.4 and an electron multiplying charge coupled device camera (Andor Technologies) with a pixel resolution of 160 nm. All channels were fabricated from fused silica samples with the help of e-beam lithography and CHF_3 reactive ion etching. Underneath a polymethylmethacrylate (PMMA) layer, the samples were coated with $\sim$50 nm sputtered

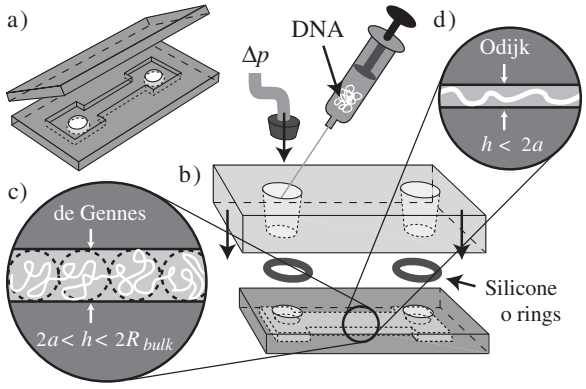

FIG. 1. Overview of the experimental setup with (a) the etched channel before bonding, (b) the bonded channel with plexiglass holder and o rings, and (c),(d) side views of the DNA confined in channels of height h in different regimes.

chromium to prevent charging during e-beam writing. Pattern transfer was done with a standard wet chromium etch. All channels connected two macroscopic filling points, 5 mm apart. The deeper channels had a uniform height over the full length, while channels with heights smaller than 90 nm only spanned a length of $\sim$200 μm, in order to ease filling. These short channels were connected to the filling points via 1–2 μm deep channels. We closed the channels by bonding them to a 200 μm thick fused silica plate, using either a silicate layer [11] or direct glass bonding [12]. In Fig. 1 a schematic picture of the setup is shown. DNA was flushed into a channel using a pressure-driven flow and stalled in the field of view of the camera. Residual flows of less than 1 $\mu\mathrm{m\,s^{-1}}$ were subtracted in the analysis. We took videos of $\sim$600 frames of $\sim$100 different molecules per channel at 20–50 Hz.

Typical images of DNA molecules are shown in Fig. 2. In the deep channels (top), we see that DNA formed fairly compact blobs, whereas in the shallow channels (bottom), the molecules were spatially more extended and also more anisotropic. In the gray scale images, broken molecules were identified on the basis of their integrated intensity $M = \sum_i I_i$ and excluded from further analysis. The conformation of the DNA molecule can be found from its gray value-weighted gyration matrix G [13],

$$G = \frac{1}{2M^2} \sum_{i,j=1}^{N} I_i I_j \begin{bmatrix} (x_i - x_j) \\ (y_i - y_j) \end{bmatrix} \begin{bmatrix} (x_i - x_j) \\ (y_i - y_j) \end{bmatrix}^T, \quad (1)$$

where I_i is the fluorescence intensity of pixel i above the background, and where indices i and j run across all N pixels of the molecule. The eigenvalues of G correspond to the axes of maximal and minimal moment of inertia. For a homogeneous ellipse, these moments equal $R_M^2/4$ and $R_m^2/4$, with R_M and R_m the radii of the ellipse along its principal axes, denoted major and minor axis, respectively. Hence

$$R_M = 2\sqrt{\lambda_1} \quad \text{and} \quad R_m = 2\sqrt{\lambda_2}, \quad (2)$$

with λ_i the eigenvalues of G (see the inset of Fig. 3 for an illustration). The projection of the radius of gyration of the molecule parallel to the confining planes, denoted $R_\parallel$, is given by

$$R_\parallel = \sqrt{(R_M^2 + R_m^2)/2}. \quad (3)$$

Figure 3 shows the measured distributions of the major and minor axes for λ DNA in a 107 nm high channel. Both distributions are clearly non-Gaussian due to their fat tails at large extension values. The asymmetry of the distributions can be understood as follows. The conformation of the DNA molecule is mainly determined by two terms: the elastic bending energy and the excluded volume effect. For the elastic term, we can take the result from an ideal chain, where the elastic free energy F_{el} is given by [14]

$$\frac{F_{\mathrm{el}}}{k_B T} \sim \frac{R^2}{Na^2}, \quad (4)$$

with T the temperature, k_B the Boltzmann constant, and N the number of monomers. The chain extension R corresponds to either R_M or R_m. In a mean field approximation, the repulsive contribution F_{rep} of the excluded volume interactions to the free energy depends on the internal monomer concentration c as $F_{\mathrm{rep}} \sim \langle c \rangle^2$ [14]. In our quasi-two-dimensional confinement, F_{rep} scales as

$$\frac{F_{\mathrm{rep}}}{k_B T} \sim \frac{N^2}{h(R - R_{\mathrm{min}})^2}, \quad (5)$$

with R_{min} the size of the most tightly packed configuration of the monomers. From Eqs. (4) and (5), the distribution of R should obey

$$P(R) \sim e^{-R^2/\sigma_1} e^{-\sigma_2/(R-R_{\mathrm{min}})^2}, \quad (6)$$

where σ_1 and σ_2 depend on N, a, and the proportionality constants in Eqs. (4) and (5). The distribution of Eq. (6) fits the distributions of R_M and R_m with remarkable accuracy at every confinement; see the solid lines in Fig. 3. The fit to the data of Fig. 3 yields $R_{\mathrm{min}} = 0.37 \pm 0.1$ μm.

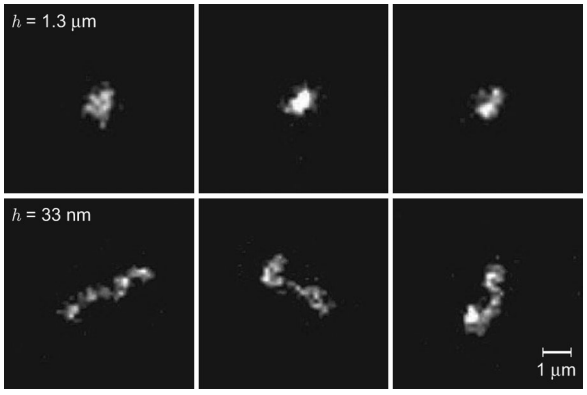

FIG. 2. Typical images of λ DNA in 1.3 μm and 33 nm high channels.

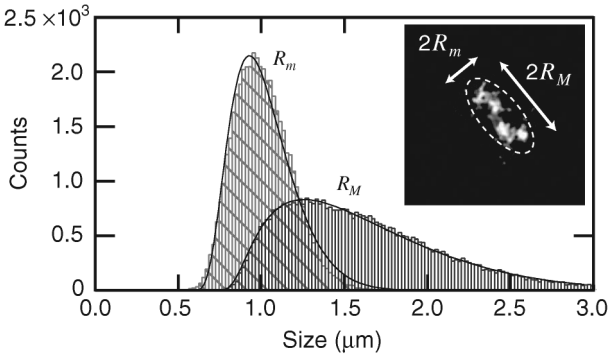

FIG. 3. Histograms of the size of the major axis (R_M) and the minor axis (R_m) where $h = 107$ nm. Solid lines are fits of Eq. (6). In the inset a snapshot of a molecule is shown with R_M and R_m as calculated with Eqs. (1) and (2).

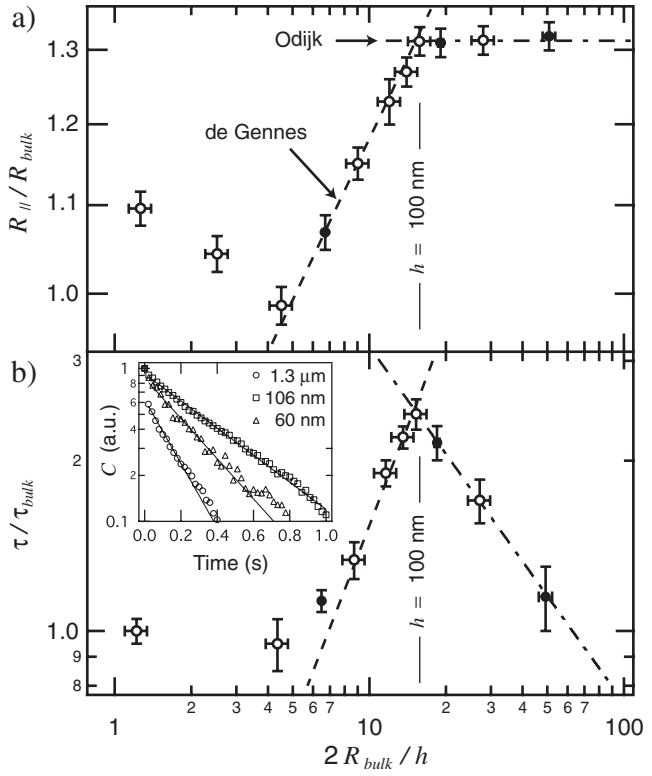

FIG. 4. Dependence of polymer extension and relaxation time on confinement in a slitlike nanochannel, with (a) the radius of gyration parallel to the channel walls, scaled by its bulk value of 0.84 μm. The dashed line represents the scaling of Eq. (7), while the dash-dotted line is a fit to the points in the Odijk regime. Data points indicated with open circles were measured in channels that were bonded using silicate bonding, while the solid circles represent the directly bonded channels. (b) The relaxation time, scaled by its bulk value of 0.2 s. The dashed line represents the scaling of Eq. (8), and the dash-dotted line denotes $\tau \sim (R_{\mathrm{bulk}}/h)^{-0.63}$. In the inset, time autocorrelation functions C of $R_\parallel$ are shown for different channel heights, fitted with exponential functions.

Since the scaling theory on molecular size is based on optimization of the free energy, R_M and R_m are taken from the peaks of the distributions of Fig. 3. Figure 4(a) shows $R_\parallel$, calculated with Eq. (3), plotted as a function of the confinement $2R_{\mathrm{bulk}}/h$.

We measured the radius of gyration in bulk, where the molecules were floating between two glass slides more than 10 μm apart, giving $R_{\mathrm{bulk}} = 0.84 \pm 0.1$ μm. This corresponds well to the literature value of 0.73 μm [15], considering the point spread function of the optical system. The data in Fig. 4(a) were scaled by this measured bulk radius. At $h \approx 2R_{\mathrm{bulk}}$, $R_\parallel$ is actually larger than its bulk value, which we ascribe to orientation of the ellipsoid with its major axes parallel to the confining planes. Upon further confinement, the coil is compressed, leading to a decrease of all principal axes. This counterintuitive behavior, of which this is the first experimental observation, has both been seen in simulations [16] and derived analytically [17]. When the polymer is confined to less than a quarter of its bulk diameter, excluded volume interactions take over, and the chain starts extending in the directions parallel to the confining planes. We fitted the function $R_\parallel \sim (R_{\mathrm{bulk}}/h)^\alpha$ to the data points in this de Gennes regime, giving $\alpha = 0.23 \pm 0.03$. Daoud and de Gennes [18] predict a scaling of $R_\parallel$ of this semi-two-dimensional polymer coil with confinement,

$$R_\parallel \sim aN^{3/5}(R_{\mathrm{bulk}}/h)^{1/4}. \quad (7)$$

In Fig. 4(a), the scaling of Eq. (7) is shown as a dashed line. Evidently, the de Gennes scaling holds nicely until $h \approx 100$ nm. At $h \approx 100$ nm, the curve shows a sharp discontinuity, after which the radius of gyration becomes independent of the channel height. Theoretically, at $h \approx 2a$, the short-scale orientational freedom is restricted, and the polymer enters the Odijk regime. From the channel height at which the transition to the Odijk regime occurs, we can roughly estimate the persistence length. The perturbation of the short-scale orientational freedom starts when a DNA segment bent over an angle π just fits in the height of the channel. Since the persistence length corresponds to the length over which the DNA can bend over 1 rad on thermal energy, an estimate of the persistence length gives $a \approx 50$ nm. This value is compatible with the literature value of the persistence length of DNA of ~66 nm, although recent measurements indicate lower values [19,20].

To first order, the dynamics of the DNA can be described by the relaxation time of the first normal mode. We have measured this relaxation time by fitting an exponential function to the autocorrelation function C of the variation from the mean of the radius of gyration, $C(j) = \frac{1}{N-j} \times \sum_{i=0}^{N-j-1}[R_\parallel(i) - \bar{R}_\parallel][R_\parallel(i+j) - \bar{R}_\parallel]$, with $\bar{R}_\parallel$ the average of $R_\parallel$. Some examples are shown in the inset of Fig. 4(b). The exponent is found to be identical for the autocorrelation functions C of each of the quantities R_M, R_m, and $R_\parallel$, as expected. In Fig. 4(b), we have plotted the relaxation time τ, scaled by its literature bulk value $\tau_{\mathrm{bulk}} = 0.2$ s [21], as a function of the confinement. Up to a confinement of $2R_{\mathrm{bulk}}/h \approx 5$, the relaxation time is close to its bulk value, after which it increases strongly. A scaling theory for τ can be easily found from balancing an internal friction coefficient ζ and an effective spring constant k as $\tau = \zeta/k$. For the de Gennes regime [22]

$$\tau \sim (R_{\mathrm{bulk}}/h)^{7/6}. \quad (8)$$

Up to a confinement to $h \approx 100$ nm, the scaling of Eq. (8) [dashed line in Fig. 4(b)] holds within experimental errors. Previous measurements gave an exponent of 0.9 [23]. In the Odijk regime, the relaxation time shows a strong decay. The dramatic change of the dynamical behavior occurs at the same level of confinement where the scaling of the radius of gyration changes, which is a strong indication of the transition to the Odijk regime. In Fig. 4(b), we fitted the data with the scaling relation $\tau \sim (R_{\mathrm{bulk}}/h)^\alpha$, giving $\alpha = -0.63 \pm 0.05$. A similar decrease was reported previously for tubelike confinement [6]. Following the theoretical

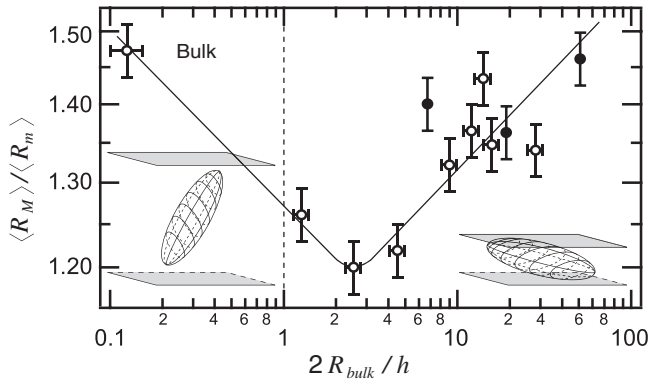

FIG. 5. Anisotropy of the molecules as a function of confinement, with symbols as in Fig. 4. The solid line is a guide to the eye. The confinement of the bulk measurement is an estimate based on the amount of liquid used and the size of the glass plates. In the insets, an ellipsoidal polymer coil is depicted schematically in bulk (left) and in confinement (right).

analysis in Ref. [6], the spring constant is expected to be independent of h, because the change in k is due only to the change of the equilibrium extension. Because ζ hardly depends on the confinement either [24,25], the relaxation time is predicted to depend only weakly on the confinement [26], contrary to our observation. The decrease in τ is observed in both the silicate-bonded channels and the direct-bonded channels, indicating that the influence of the particularities of the channel wall is minor.

We finally report the shape anisotropy of DNA, which we define as $\langle R_M \rangle / \langle R_m \rangle$. Figure 5 shows the anisotropy as a function of confinement. In the confined regime, the two largest principal axes of the polymer coil are oriented parallel to the confining planes; see the right-hand side of Fig. 5. The anisotropy is consequently determined by the ratio of these two axes. In bulk, however, the molecule can also project its shortest principal axis onto an image, so three possible aspect ratios contribute to the average anisotropy, increasing its value as seen at the left in Fig. 5. Theoretical values of the anisotropy of flexible polymers range from 2.8 in bulk to 2.2 at $h \approx R_{\mathrm{bulk}}$ [16] and 2.6 for a two-dimensional random walk [27]. Qualitatively, the general shape of the curve complies with theory, but numerically, the anisotropy is significantly lower than predicted. We have checked our measurement method by analyzing images of metal ellipses of different aspect ratios, giving the correct values. Previous measurements of the anisotropy of DNA molecules in bulk gave a value of $\sim 2.2 \pm 0.7$ [28], using a different method.

In conclusion, we observe three different regimes of the scaling of molecule size and relaxation dynamics with confinement. The transitions occur at the predicted confinement levels. Our measurements agree with theory down to a channel height of 100 nm. In the Odijk regime, the radius of gyration remains constant and the relaxation time decreases drastically. The anisotropy of DNA appears to be lower than predicted from random walks.

We thank T. Odijk for helpful discussions, F. van der Heyden and R. Driessen for their help, A. van den Berg and S. Pennathur for advice on the channel fabrication, and FOM, NWO, and NanoNed for financial support.

*Present address: Physik Department, Technische Universität München, James Franck Straße, 85748 Garching, Germany.
†Present address: Brown University, 182 Hope Street, Providence, RI 02912, USA.
‡Corresponding author.

[1] K. Jo *et al.*, Proc. Natl. Acad. Sci. U.S.A. **104**, 2673 (2007).
[2] W. D. Volkmuth and R. H. Austin, Nature (London) **358**, 600 (1992).
[3] M. C. Williams, Proc. Natl. Acad. Sci. U.S.A. **104**, 11 125 (2007).
[4] S. Jun and B. Mulder, Proc. Natl. Acad. Sci. U.S.A. **103**, 12 388 (2006).
[5] D. Stein *et al.*, Proc. Natl. Acad. Sci. U.S.A. **103**, 15 853 (2006).
[6] W. Reisner *et al.*, Phys. Rev. Lett. **94**, 196101 (2005).
[7] J. O. Tegenfeldt *et al.*, Proc. Natl. Acad. Sci. U.S.A. **101**, 10 979 (2004).
[8] B. Maier and J. O. Rädler, Phys. Rev. Lett. **82**, 1911 (1999).
[9] J. Han and H. G. Craighead, Science **288**, 1026 (2000).
[10] S. R. Quake, H. Babcock, and S. Chu, Nature (London) **388**, 151 (1997).
[11] D. Stein, M. Kruithof, and C. Dekker, Phys. Rev. Lett. **93**, 035901 (2004).
[12] S. C. Jacobson, A. W. Moore, and J. M. Ramsey, Anal. Chem. **67**, 2059 (1995).
[13] D. N. Theodorou and U. W. Suter, Macromolecules **18**, 1206 (1985).
[14] P. G. de Gennes, *Scaling Concepts in Polymer Physics* (Cornell University, Ithaca, 1979).
[15] D. E. Smith, T. T. Perkins, and S. Chu, Macromolecules **29**, 1372 (1996).
[16] J. H. van Vliet, M. C. Luyten, and G. ten Brinke, Macromolecules **25**, 3802 (1992).
[17] C. E. Cordeira, M. Molisano, and D. Thirumalai, J. Phys. II (France) **7**, 433 (1997).
[18] M. Daoud and P. G. de Gennes, J. Phys. (Paris) **38**, 85 (1977).
[19] I. Vladescu *et al.*, Nat. Methods **4**, 517 (2007).
[20] A. Sischka *et al.*, Biophys. J. **88**, 404 (2004).
[21] G. C. Randall and P. S. Doyle, Phys. Rev. Lett. **93**, 058102 (2004).
[22] F. Brochard, J. Phys. (Paris) **38**, 1285 (1977).
[23] C. Hsieh, A. Balducci, and P. S. Doyle, Macromolecules **40**, 5196 (2007).
[24] M. Doi and S. F. Edwards, *The Theory of Polymer Dynamics* (Oxford University, Oxford, 1986).
[25] O. B. Bakajin *et al.*, Phys. Rev. Lett. **80**, 2737 (1998).
[26] T.Odijk (private communication).
[27] M. Bishop and C. Saltiel, J. Chem. Phys. **85**, 6728 (1986).
[28] C. Haber, S. Ruiz, and D. Wirtz, Proc. Natl. Acad. Sci. U.S.A. **97**, 10 792 (2000).